Polarization readout analysis for multilevel phase change recording by crystallization degree modulation*

Lin Jin-Cheng(林金成)[a)b)], Long Guo-Yun(龙国云)[a)b)], Wang Yang(王 阳)[a)†], and Wu Yi-Qun(吴谊群)[a)]

[a)] *Key Laboratory of High Power Laser Materials, Shanghai Institute of Optics and Fine Mechanics, Chinese Academy of Sciences, Shanghai* 201800, *China*
[b)] *University of the Chinese Academy of Sciences, Beijing* 100049, *China*

(Received 18 March 2013; revised manuscript received 8 April 2013)

Four different states of $Si_{15}Sb_{85}$ and $Ge_2Sb_2Te_5$ phase change memory thin films are obtained by crystallization degree modulation through laser initialization at different powers or annealing at different temperatures. The polarization characteristics of these two four-level phase change recording media are analyzed systematically. A simple and effective readout scheme is then proposed, and the readout signal is numerically simulated. The results show that a high-contrast polarization readout can be obtained in an extensive wavelength range for the four-level phase change recording media using common phase change materials. This study will help in-depth understanding of the physical mechanisms and provide technical approaches to multilevel phase change recording.

Keywords: optical data storage, phase change memory materials, multilevel recording, polarization readout

PACS: 42.70.Ln, 42.79.Vb **DOI:** 10.1088/1674-1056/22/12/124208

1. Introduction

Traditional data storage is realized through binary (two-level) coding, that is, the unmarked and marked states corresponding to level 0 and level 1 respectively. It means that one bit can be recorded with a recording mark (cell) if the coding efficiency is not taken into consideration. Numerous attempts have been made to increase the recording density through multilevel recording.[1,2] It means that each recording mark (cell) can record $\log_2 L$ bits, where L is the number of levels. For example, a four-level recording gives $\log_2 4 = 2$ bits per mark (cell) and doubles the recording density.

Multilevel phase change recording was first reported by Ovshinsky in his early work[3] and continued refinements later.[4] The intermediate reflectivity or resistivity levels can be obtained by mark size modulation,[5,6] partial crystallization effect,[7,8] stacked structure,[9–12] etc. Although it is simple in principle, the multilevel recording, such as recording and readout of the multilevel signals in the existing or improved operation systems, remains challenging in its implementation.

As is well known, the maximum difference in electrical resistivity (or conductivity) between amorphous and crystalline states can be approximately four orders to six orders in magnitude, which can result in more levels and higher contrast for readouts. On the contrary, the optical reflectivity contrast between amorphous and crystalline states is commonly about 10% to 30%. The number of multi levels will be greatly limited by reflective intensity detection. Therefore, finding other ways to read out the difference of optical signals with high contrast is very important for multi-level phase change recording.

In fact, except the light intensity, the polarization of light has often been used to read out the recorded signals. The magneto–optical Kerr readout is one of the typical examples that detect the polarization of light.[13] Shimazaki *et al.*[14] reported that the magnetic multivalued recording in a magneto–optical disk using an exchange coupled bilayer had four magnetization states. Tsuru and Yamamoto[15] proposed a new concept of multilevel read-only-memory by arrays of multi-directional V-shape pits on an Si wafer. It changes the polarization of light by different "V-directions" of "V-pits", which can achieve 7 bits recording at each single V-pit. Yasui and Saiki[16] proposed a new reading method based on polarization-sensitive reading for high-density optical disks. The sub-diffraction-limited recording mark patterns can be read out by detecting the change in the polarization of the reflected light in addition to its intensity. Xiang and Chou[17] reported a method to differentiate the two basic levels (amorphous and crystalline states) of Te-doped $GeSb_9$ film through the polarization angle calculated from the ellipsometer data, which theoretically reveals the potential for multilevel phase change recording.

The above research achievements have shown the advantage and feasibility of polarization readout for multilevel recording. However, in-depth understanding of the mechanism and technical approach to polarization readout for the real multileveled phase change recording media is still far from enough.

In this paper, four different states of $Si_{15}Sb_{85}$ and

*Project supported by the National Natural Science Foundation of China (Grant Nos. 61178059 and 61137002) and the Key Program of the Science and Technology Commission of Shanghai Municipality, China (Grant No. 11jc1413300).

†Corresponding author. E-mail: ywang@siom.ac.cn

© 2013 Chinese Physical Society and IOP Publishing Ltd

$Ge_2Sb_2Te_5$ phase change memory thin films are obtained by crystallization degree modulation through laser initialization at different powers or annealing at different temperatures. The polarization characteristics of these two four-level phase change recording media are analyzed theoretically. An optical-pickup-compatible readout scheme is then proposed and the readout signal is simulated numerically. The results show that a high-contrast polarization readout can be obtained in a large wavelength range for the four-level phase change recording media using common phase change materials.

2. Principle of polarization readout

When a linear polarized light irradiates obliquely on the interface between two mediums, the reflected light usually becomes an elliptically polarized light as shown in Fig. 1(a). To analyze the polarization property of the reflected light, it is convenient to decompose the incident light into two independent components, the *s* light and the *p* light, of which the polarizations are perpendicular to each other. The *s* oscillation and *p* oscillation are the intrinsic oscillations of the interface between the two transparent media. An ellipsometer can be used to detect two polarization-related parameters of the material, $\tan\Psi$ and Δ, which represent the relative amplitude attenuation and the relative phase difference between *p* and *s* directions after reflection, respectively. The relationship between the two ellipsometric parameters and the complex Fresnel reflection coefficients $\tilde{r}_s$ ($\tilde{r}_s = r_s e^{i\delta_s}$) and $\tilde{r}_p$ ($\tilde{r}_p = r_p e^{i\delta_p}$) of *s* and *p* light can be expressed as

$$\tan\Psi = r_p/r_s, \tag{1}$$

$$\Delta = \delta_p - \delta_s, \tag{2}$$

where r_s and r_p are the amplitude of reflected wave for unit incident amplitude, and δ_s and δ_p are the phase changes at the interface for *s* and *p* components, respectively.

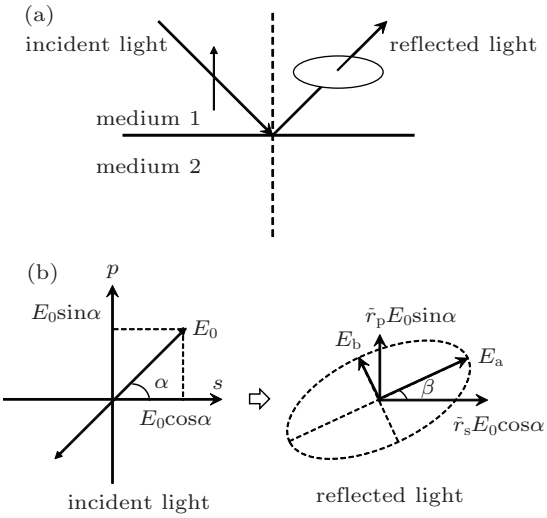


Fig. 1. Schematics of the variation of polarization state for the incident linear polarized light before and after reflection.

Usually the major axis of the reflected elliptically polarized light has a rotation angle θ with respect to the polarized direction of the incident linearly polarized light. We assume that the angle between the polarized direction of the incident light and the *s* direction is α ($-\pi/2 \leqslant \alpha < \pi/2$), and the angle between the major axis of reflected light and the *s* direction is β ($-\pi/2 \leqslant \beta < \pi/2$) as shown in Fig. 1(b). In this figure, E_0 is the electric intensity of the incident light, whereas E_a and E_b are the electric intensities of the two components along the major and minor axis of the reflected light, respectively. We introduce an auxiliary angle χ as

$$\mp\frac{E_b}{E_a} = \tan\chi. \tag{3}$$

The sign of χ reflects whether the elliptically polarized light is of levorotation or dextrorotation. Defining ε as the ratio between the minor and major axes, that is, the ellipticity, we have

$$\varepsilon = |\tan\chi|. \tag{4}$$

According to the wave theory of light, we have the relationships expressed as[18]

$$\tan 2\beta = \frac{2\tan\alpha\tan\Psi}{1-\tan^2\alpha\tan^2\Psi}\cos\Delta, \tag{5}$$

$$\sin 2\chi = \frac{2\tan\alpha\tan\Psi}{1+\tan^2\alpha\tan^2\Psi}\sin\Delta. \tag{6}$$

When α is equal to 45°, $\tan\alpha$ will be equal to 1. Thus, equations (5) and (6) can be simplified into

$$\tan 2\beta = \frac{2\tan\Psi}{1-\tan^2\Psi}\cos\Delta, \tag{7}$$

$$\sin 2\chi = \frac{2\tan\Psi}{1+\tan^2\Psi}\sin\Delta. \tag{8}$$

We can calculate out β and χ by Eqs. (7) and (8) through the ellipsometer data ($\tan\Psi$ and $\cos\Delta$). Then the polarization rotation angle θ can be given as

$$\theta = \alpha - \beta = 45^\circ - \beta, \tag{9}$$

and the ellipticity ε can be given by Eq. (4).

It should be pointed out that in our derivations, the elliptically polarized light is directly synthesized by the *p* and *s* components instead of the levorotation and dextrorotation components.[17] Thus, the limiting conditions of θ and ε (θ and ε should be very small) do not need to comply with those in Ref. [18]. As can be seen from the following experimental results, θ and ε of common phase change materials are not small enough to obey Eq. (3) in Ref. [17].

3. Polarization analysis of crystallization degree modulated phase change materials

To investigate the polarization characteristics of phase change materials in different states and evaluate the feasibility of multilevel phase change recording, four different states

of $Si_{15}Sb_{85}$[19,20] and $Ge_2Sb_2Te_5$[21,22] phase change memory thin films were obtained by crystallization degree modulation through laser initialization or annealing. The phase change thin films were prepared by magnetron sputtering in an Ar atmosphere of 0.85 Pa with an Ar flow rate of 80 sccm. The required base pressure in vacuum chambers was 6.4×10^{-4} Pa. The $Si_{15}Sb_{85}$ films were deposited on polycarbonate substrates and were initialized by a continuous wave laser (wavelength: 810 nm, spot size: 1×192 μm) with powers of 400, 800, and 1200 mW. While the $Ge_2Sb_2Te_5$ films were deposited on Si substrates and thermally annealed at the temperatures of 200, 250, and 300 °C. A Sopra GES5E UV/Vis/IR spectral ellipsometer was used to measure the ellipsometric parameters ($\tan\Psi$ and $\cos\Delta$) of the films in the wavelength region between 250 nm and 850 nm. The measurements of $Si_{15}Sb_{85}$ films were made at the incident angle of 75°, whereas the measurements of $Ge_2Sb_2Te_5$ films were made at three incident angles: 65°, 70°, and 75°.

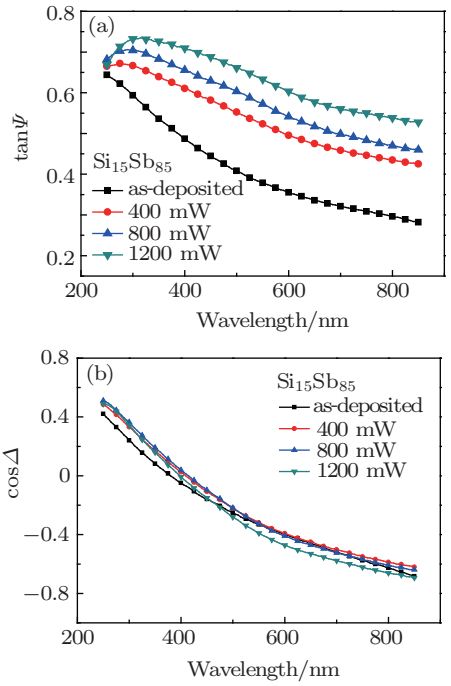


Fig. 2. (color online) Ellipsometric parameters $\tan\Psi$ (a) and $\cos\Delta$ (b) of $Si_{15}Sb_{85}$ thin films at different laser initialization powers. The incident angle is 75°.

Figure 2 shows the ellipsometric parameters of $Si_{15}Sb_{85}$ films at different laser initialization powers. Figure 3 shows the ellipsometric parameters of $Ge_2Sb_2Te_5$ films at different annealed temperatures. Their incident angles were all 75°. From Fig. 2 and Fig. 3, we can see that the variation trends of $\tan\Psi$ and $\cos\Delta$ for the $Si_{15}Sb_{85}$ films are similar to those for the $Ge_2Sb_2Te_5$ films. Both $\tan\Psi$ and $\cos\Delta$ decrease with the increase of wavelength almost in the whole wavelength range. An obvious variation is observed in $\tan\Psi$ when the crystallization degree of the films changes. By contrast, $\cos\Delta$ was almost insensitive to the crystallization degree. Thus, from Eqs. (7) and (9), we can roughly infer that the polarization rotation angle θ will have considerable variations at different crystallization degrees.

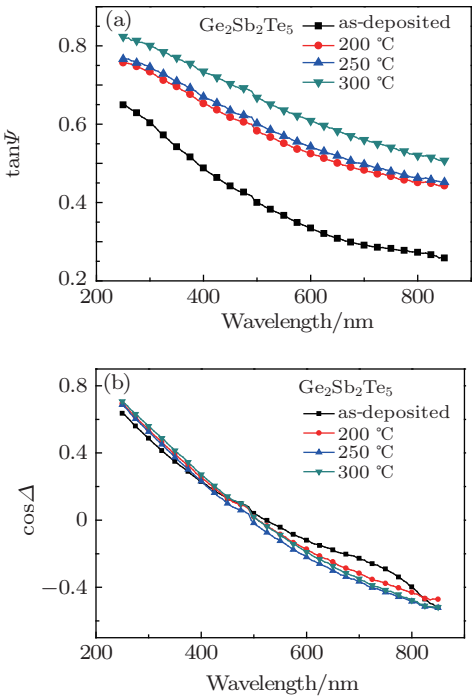


Fig. 3. (color online) Ellipsometric parameters $\tan\Psi$ (a) and $\cos\Delta$ (b) of $Ge_2Sb_2Te_5$ thin films at different annealing temperatures. The incident angle is 75°.

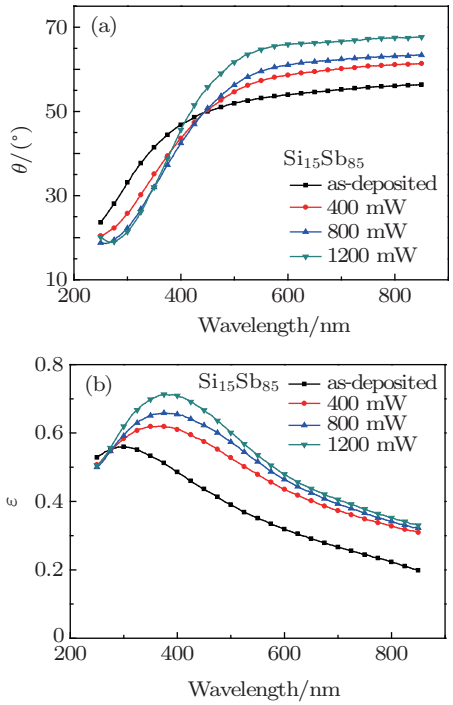


Fig. 4. (color online) Plots of polarization rotation angle θ (a) and ellipticity ε (b) versus wavelength of $Si_{15}Sb_{85}$ films at different laser initialization powers. The incident angle is 75°.

From the ellipsometric parameters, the polarization rotation angle θ and the ellipticity ε can be calculated out. Figure 4(a) shows the variations of polarization rotation angle θ

with wavelength of the $Si_{15}Sb_{85}$ films at different laser initialization powers. From Fig. 4(a), we can see that θ is almost independent of the wavelength after 500 nm. Moreover, θ increases with the laser initialization power after 500 nm but the reverse trend appears before 400 nm. The difference in θ between different laser initialization powers after 500 nm was large, ranging from 2° to 6°. The smallest difference in θ between 400 mW and 800 mW is approximately 2° to 3°. Figure 4(b) shows the variations of ellipticity ε with wavelength of the reflected elliptically polarized light for the $Si_{15}Sb_{85}$ films at different laser initialization powers. From Fig. 4(b), we can see that ε first increases and then decreases with increasing wavelength. The value of ε is smaller than 0.5 after 500 nm, and decreases to 0.3 in the near infrared region.

The variations of polarization rotation angleθ with wavelength of $Ge_2Sb_2Te_5$ films at different annealing temperatures and incident angles (65° , 70° and 75°) are shown in Figs. 5(a)–5(c). Since the reflection coefficient is related to the incident angle, the polarization rotation angle will vary with the incident angle. From Fig. 5(a)–5(c), we can see that the differences in θ between different annealing temperatures for $Ge_2Sb_2Te_5$ film increase with the incident angle. This phenomenon is more obvious in the red and infrared regions. When the incident angle is 75°, the difference of θ in the wavelength region of 650 nm–850 nm reaches 2° between two adjacent states as shown in Fig. 5(c). Moreover, we notice that the ellipticity ε shown in Fig. 5(d) is smaller than 0.5 in the wavelength region between 700 nm and 850 nm.

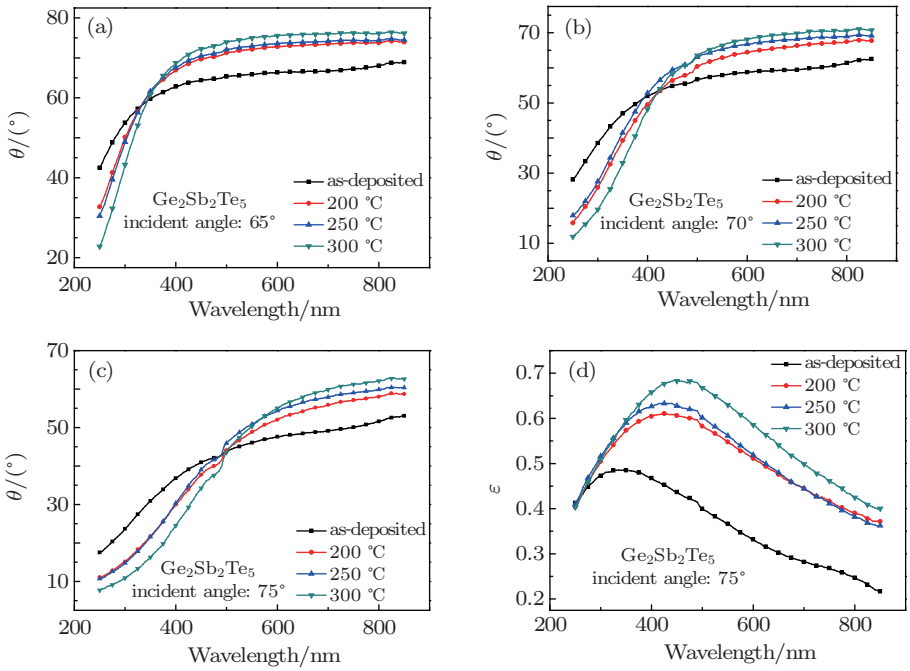


Fig. 5. (color online) Plots of polarization rotation angle θ versus wavelength of $Ge_2Sb_2Te_5$ films at different annealing temperatures and incident angles of 65° (a), 70° (b) and 75° (c), and the plots of ellipticity ε versus wavelength of $Ge_2Sb_2Te_5$ films at different annealing temperatures and an incident angle of 75° (d).

With a large difference of θ and a minor ε in a certain wavelength range (for example, in a range of 500 nm–850 nm), the different crystallization degree modulated states can be easily differentiated by detecting the polarization angle of the reflected light.

4. Readout scheme and signal analysis for multilevel phase change recording

The detectable differences between polarization rotation angles at different crystallization degree modulated states provide the possibility of recording the multilevel phase change. The multilevel recording can be carried out by pulse width and power modulation,[9] But how can it be read out? After all, an ellipsometer cannot be used as a normal readout system for practical data storage. It is important to design an optical-pickup-compatible readout system for practical applications.

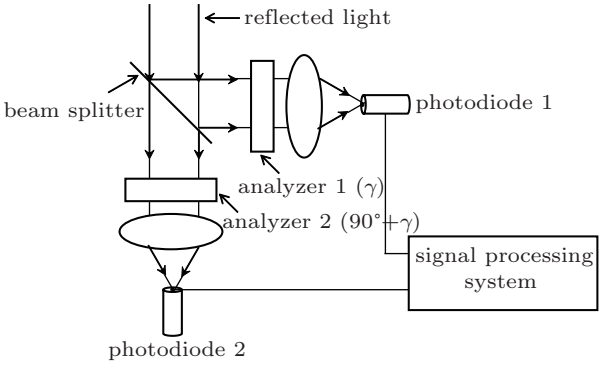


Fig. 6. Readout scheme for multilevel phase change recording.

The most direct method is to use an analyzer based on the Malus law, which can be easily integrated into a compact optical head. Here a readout scheme is proposed based on it as shown in Fig. 6. The reflected light passes through a beam splitter with a 50:50 splitting ratio and splits into two halves with the same intensity. Then the two beams pass through two analyzers respectively. The two analyzers are identical except for the azimuthal angles (the angle between the transmission direction of the analyzer and the s direction). One is set to be γ ($-\pi/2 \leqslant \gamma < \pi/2$), and the other is set to be $90^\circ + \gamma$. Here γ is a key parameter to achieve optimal readout effect. The light intensity is detected by two photodiodes and the output signal is obtained by dividing the two signals.

We define $\boldsymbol{a}_\mathrm{s}$ and $\boldsymbol{a}_\mathrm{p}$ as the unit vectors along s and p directions, respectively. From Fig. 1(b), we obtain the following expression since $\alpha = 45^\circ$:

$$\begin{aligned}&\frac{\sqrt{2}}{2}E_0\left(\tilde{r}_\mathrm{s}\boldsymbol{a}_\mathrm{s}+\tilde{r}_\mathrm{p}\boldsymbol{a}_\mathrm{p}\right)\\ =&\left[E_\mathrm{a}\left(\cos\beta\boldsymbol{a}_\mathrm{s}+\sin\beta\boldsymbol{a}_\mathrm{p}\right)\right.\\ &\left.+E_\mathrm{b}\exp\left(\pm\frac{\mathrm{i}\pi}{2}\right)\left(\sin\beta\boldsymbol{a}_\mathrm{s}-\cos\beta\boldsymbol{a}_\mathrm{p}\right)\right]\exp(\mathrm{i}\varphi),\end{aligned}\tag{10}$$

in which φ is a constant phase angle, the sign of $\pi/2$ determines the direction of rotation around the ellipse. From Eq. (10) we obtain

$$\tilde{r}_\mathrm{s}=\frac{\sqrt{2}E_\mathrm{a}}{E_0}\exp(\mathrm{i}\varphi)(\cos\beta\pm\mathrm{i}\varepsilon\sin\beta),\tag{11}$$

$$\tilde{r}_\mathrm{p}=\frac{\sqrt{2}E_\mathrm{a}}{E_0}\exp(\mathrm{i}\varphi)(\sin\beta\mp\mathrm{i}\varepsilon\cos\beta).\tag{12}$$

Then the reflected light can be expressed by the Jones matrix as

$$\boldsymbol{E}_\mathrm{r}=\begin{bmatrix}\frac{\sqrt{2}}{2}\tilde{r}_\mathrm{s}E_0\\ \frac{\sqrt{2}}{2}\tilde{r}_\mathrm{p}E_0\end{bmatrix}=E_\mathrm{a}\exp(\mathrm{i}\varphi)\begin{bmatrix}\cos\beta\pm\mathrm{i}\varepsilon\sin\beta\\ \sin\beta\mp\mathrm{i}\varepsilon\cos\beta\end{bmatrix}.\tag{13}$$

The Jones matrix of an analyzer with the azimuthal angle γ is

$$\boldsymbol{J}_\mathrm{a}=\begin{bmatrix}\cos^2\gamma & \sin\gamma\cos\gamma\\ \sin\gamma\cos\gamma & \sin^2\gamma\end{bmatrix}.\tag{14}$$

Thus the Jones matrix of the beam after transmission through analyzer 1 is

$$\begin{aligned}\boldsymbol{E}_1 &= \frac{\sqrt{2}}{2}\boldsymbol{J}_\mathrm{a}\boldsymbol{E}_\mathrm{r}=\frac{\sqrt{2}}{2}E_\mathrm{a}\exp(\mathrm{i}\varphi)\\ &\times\begin{bmatrix}\cos\gamma\cos(\beta-\gamma)\pm\mathrm{i}\varepsilon\cos\gamma\sin(\beta-\gamma)\\ \sin\gamma\cos(\beta-\gamma)\mp\mathrm{i}\varepsilon\sin\gamma\sin(\beta-\gamma)\end{bmatrix}.\end{aligned}\tag{15}$$

The factor of $\sqrt{2}/2$ is attributed to the light division by the beam splitter. The intensity of the beam is

$$I_1=|\boldsymbol{E}_1|^2=\frac{1}{2}E_\mathrm{a}^2[\cos^2(\beta-\gamma)+\varepsilon^2\sin^2(\beta-\gamma)].\tag{16}$$

Analogously, the intensity of the beam after transmission through analyzer 2 is

$$I_2=\frac{1}{2}E_\mathrm{a}^2[\sin^2(\beta-\gamma)+\varepsilon^2\cos^2(\beta-\gamma)].\tag{17}$$

The readout signal S is the ratio between I_2 and I_1, which is given as

$$S=\frac{I_2}{I_1}=\frac{\tan^2(\beta-\gamma)+\varepsilon^2}{1+\varepsilon^2\tan^2(\beta-\gamma)}.\tag{18}$$

Figure 7 shows the curves of the readout signal S versus $\tan(\beta-\gamma)$ with different value of ε. We can see that S is almost insensitive to ε in the area near $\tan(\beta-\gamma)=1$, which is marked by the square in Fig. 7. Since ε varies with the crystallization degree of the film, it is appropriate to adjust the value of γ to make $\tan(\beta-\gamma)$ equal to approximately 1 (namely, $\beta-\gamma\approx 45^\circ$). In addition, from Fig. 7 we can see that the point of $\tan(\beta-\gamma)=1$ is near the inflection point of the curve, thus suggesting better distinction of the readout signal for different β values when $\tan(\beta-\gamma)$ is approximately 1.

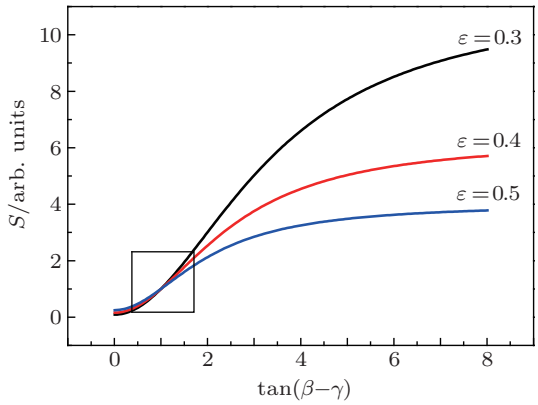


Fig. 7. (color online) Curves of read out signal S versus $\tan(\beta-\gamma)$ with $\varepsilon = 0.3, 0.4, 0.5$.

In the actual operation, the value of β of any one intermediate level (not the initial or final level) should be first determined by the analyzer or ellipsometer, and then the value of γ is adjusted to make $\beta-\gamma\approx 45^\circ$. The optimal readout effect can be easily obtained under this condition.

With the data of β and ε obtained from the ellipsometric parameters, we can calculate out the values of readout signal S for the crystallization degree modulated $Si_{15}Sb_{85}$ and $Ge_2Sb_2Te_5$ films within the wavelength range between 500 nm and 850 nm as shown in Figs. 8 and 9. The value of γ is adjusted to -68° and -64° for the $Si_{15}Sb_{85}$ and $Ge_2Sb_2Te_5$ films, respectively, to optimize the readout effect. If we define the signal contrast (C_S) as $C_S = 2\times|S_\mathrm{a}-S_\mathrm{c}|/(S_\mathrm{a}+S_\mathrm{c})$, where S_a is the readout signal of the as-deposited initial state (level 1), and S_c is the readout signal of the crystallized state with a certain crystallization degree (level 2, 3, 4), then the C_S of each level at a certain wavelength can be calculated out. In Table 1 are listed the values of C_S of levels 2–4 for $Si_{15}Sb_{85}$

and $Ge_2Sb_2Te_5$ films at two typical optical recording wavelengths (650 nm and 780 nm). The maximum C_S between level 1 and level 4 can reach a value larger than 60% for both materials, which is much larger than the reflectivity contrast between the amorphous and crystalline states (10%–30%). The results show that a high-contrast polarization readout can be obtained in a large wavelength range for the four-level phase change recording, which confirms the validity of the proposed readout scheme.

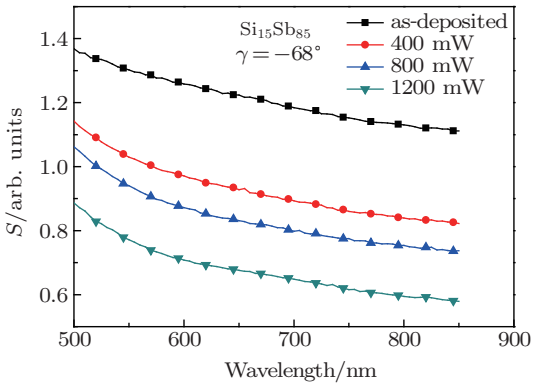


Fig. 8. (color online) Plots of readout signal S versus wavelength of $Si_{15}Sb_{85}$ films at different laser initialization powers. The value of γ is adjusted to $-68°$ for an optimal readout.

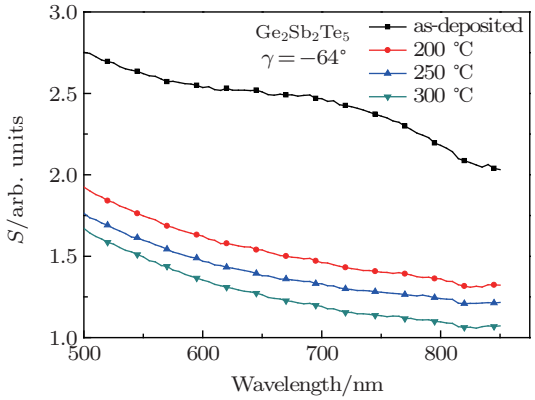


Fig. 9. (color online) Plots of readout signal S versus wavelength of $Ge_2Sb_2Te_5$ films at different annealing temperatures. The value of γ is adjusted to $-64°$ for an optimal readout.

Table 1. Signal contrasts among levels 2–4 and level 1 for $Si_{15}Sb_{85}$ and $Ge_2Sb_2Te_5$ films at wavelengths of 650 nm and 780 nm. Levels 2, 3, and 4 correspond to the crystallization degree modulated states by laser initialization at powers of 400, 800, and 1200 mW for $Si_{15}Sb_{85}$ films and by annealing at temperatures of 200, 250, and 300 °C for $Ge_2Sb_2Te_5$ films, respectively. Level 1 corresponds to the as-deposited initial state of the films.

	Level 1	Level 2	Level 3	Level 4
@650 nm ($Si_{15}Sb_{85}$)	0	27.4%	38.2%	57.7%
@650 nm ($Ge_2Sb_2Te_5$)	0	48.0%	58.0%	66.0%
@780 nm ($Si_{15}Sb_{85}$)	0	28.9%	40.0%	61.3%
@780 nm ($Ge_2Sb_2Te_5$)	0	48.6%	57.0%	68.2%

5. Conclusions

In this paper, four different states of $Si_{15}Sb_{85}$ and $Ge_2Sb_2Te_5$ phase change memory thin films are obtained by crystallization degree modulation through laser initialization at different powers or annealing at different temperatures. The polarization characteristics of these two four-level phase change recording media are analyzed systematically. The polarization rotation angle and the ellipticity of the reflected light are theoretically calculated out with the ellipsometer data. With the considerable polarization rotation angle difference and the minor ellipticity in a certain wavelength region, the different crystallization degree modulated states can be easily differentiated by detecting the polarization angle of the reflected light. A simple and effective readout scheme is then proposed, and then the readout signal is simulated numerically. The maximum signal contrast between level 1 and level 4 can reach a value larger than 60% at 780 nm for both materials, which is much larger than the traditional reflectivity contrast between the amorphous and crystalline states. The results show that a high-contrast polarization readout can be achieved in a large wavelength range for the four-level phase change recording using common phase change materials. Many more levels can be expected after the optimization of the recording media and the readout system.

References

[1] Ovshinsky S R and Czubatyj W 2001 *Proc. SPIE* **4085** 15
[2] Ohta A 2001 *J. Optoelectron. Adv. Mater.* **3** 609
[3] Ovshinsky S R 1982 *Disordered Materials: Science and Technology* (Michigan: Amorphous Institute Press) pp. 2–22
[4] Ovshinsky S R 1999 *Materials Research Society Symposium Proceedings* **554** 399
[5] Ohta T, Nishiuchi K, Narumi K, Kitaoka Y, Ishibashi H, Yamada N and Kozaki T 2000 *Jpn. J. Appl. Phys.* **39** 770
[6] Kiyono K, Horie M, Ohno T, Uematsu T, Hashizume T, Neill M P O, Balasubramanian K, Narayan R, Warland D and Zhou T 2001 *Jpn. J. Appl. Phys.* **40** 1855
[7] Shi L P, Chong T C, Tan P K, Miao X S, Huang Y M and Zhao R 1999 *Jpn. J. Appl. Phys.* **38** 1645
[8] Liu B, Zhang T, Xia J, Song Z, Feng S and Chen B 2004 *Semicond. Sci. Technol.* **19** L61
[9] Shieh H P D, Chen Y L and Wu C H 2001 *Jpn. J. Appl. Phys.* **40** 1850
[10] Xiao J X, Qi G S, She P, Liu R and Xu D Y 2003 *Chin. Phys.* **12** 1241
[11] Zhang Y, Feng J, Zhang Y, Zhang Z, Lin Y, Tang T, Cai B and Chen B 2007 *Phys. Status Solidi (RRL)* **1** R28
[12] Hu Y, Sun M, Song S, Song Z and Zhai J 2012 *Integr. Ferroelectr.* **140** 8
[13] Mansuripu M, Connell G A N and Goodman J W 1982 *J. Appl. Phys.* **53** 4485
[14] Shimazaki K, Yoshihiro M, Ishizaki O, Ohnuki S and Ohta N 1995 *Proc. Magnetic-Optical Recording International Symposium* **94** 429
[15] Tsuru T and Yamamoto M 2008 *Opt. Express* **16** 9622
[16] Yasui T and Saiki T 2011 *Jpn. J. Appl. Phys.* **50** 072502
[17] Xiang C and Chou L 2010 *Appl. Phys. Lett.* **96** 171105
[18] Born M and Wolf E 1999 *Principles of Optics* (7th *expanded edition*) (Cambridge: Cambridge University Press) pp. 25–29
[19] Zhang T, Song Z, Wang F, Liu B, Feng S and Chen B 2007 *Appl. Phys. Lett.* **91** 222102
[20] Huang H, Li S, Zhai F, Wang Y, Lai T, Wu Y and Gan F 2011 *Mater. Chem. Phys.* **128** 405
[21] Huang H, Zuo F, Zhai F, Wang Y, Lai T, Wu Y and Gan F 2009 *J. Appl. Phys.* **106** 063501
[22] Zuo F, Wang Y, Wu Y and Lai T 2009 *Acta Phys. Sin.* **58** 7250 (in Chinese)